Advances in Environmental Technology 12(3) 2026, 328-340.

Iranian Reasearch Organization for Science and Technology (IROST)

Advances in Environmental Technology

Journal home page: https://aet.irost.ir

Titanium dioxide Sol–Gel/Zinc oxide Sol–Gel and Titanium dioxide Sol–Gel/powdered Zinc Oxide-coated clay beads in photocatalytic reactor

Thurgadewi Krishnan[a]*, Maria Medina-Llamas[b], Mohamad Awang[a], Wan Rafizah Wan Abdullah[a], Wan Salida Wan Mansor[a]

[a] *Faculty of Ocean Engineering Technology, University Malaysia Terengganu, 21030 Kuala Nerus, Terengganu, Malaysia.*

[b] *Unidad Académica Preparatoria, Plantel II, Universidad Autónoma de Zacatecas, Zacatecas, Zac 98068, México.*

ARTICLE INFO

Document Type:
Research Paper

Article history:
Received 29 May 2025
Received in revised form
09 May 2026
Accepted 12 May 2026

Keywords:
Clay beads
Immobilization
Photocatalysis
Recyclability
TiO_2/ZnO

ABSTRACT

Nowadays, immobilized photocatalyst clay beads have attracted considerable research interest due to their outstanding properties, including enhanced stability, easy recovery and reuse, and reduced secondary pollution. In this study, novel titanium dioxide/zinc oxide composites were synthesized via the sol–gel method and immobilized on clay beads using the dip-coating process. Various titanium dioxide/zinc oxide ratios were used to obtain different composites. For the immobilization procedure, four titanium dioxide/zinc oxide layers were coated on clay beads, dried in the oven at 100°C for 30 min, and subsequently calcined at 2°C/min up to 500°C. The coated beads were characterized using Scanning Electron Microscopy (SEM) and Energy Dispersive Spectroscopy (EDS). Photocatalytic degradation experiments were conducted to test their performance using methylene blue as a model pollutant. The highest methylene blue degradation efficiency was achieved with pure titanium dioxide-coated clay beads. All titanium dioxide/zinc oxide composites maintained their photocatalytic performance after five consecutive recyclability experiments. This work aims to demonstrate a reproducible, scalable, and economic immobilization procedure for single and composite photocatalysts on clay beads with outstanding photocatalytic performances for wastewater treatment.

1. Introduction

There has been an ongoing interest in the photocatalytic application of semiconductors for a wide range of applications, including water disinfection [1], organic photodegradation [2], water purification [3], and epoxidation of alkenes [4]. According to Slama [5], the direct discharge of dye effluents from textile industries could trigger serious environmental problems due to their organic load and toxicity. Textile dyes such as methylene blue (MB) contain benzene rings with

*Corresponding author Tel.: +60 177367032
E-mail: k.thurgadewi@gmail.com
DOI: 10.22104/aet.2026.7571.2146

carcinogenic properties, posing risks to both human health and the environment [6]. According to Zamel and Khan [7], MB exposure can cause eye burns that may result in permanent damage to human and animal eyes. Thus, the photocatalytic application of semiconductors offers a promising strategy for mineralizing toxic substances into harmless end products [8].

The most common photocatalysts, TiO_2 and ZnO, are widely used due to their non-toxic nature, anti-bacterial properties, relatively high activity, and good physical and chemical stability [9, 10]. Each photocatalyst has its own intrinsic advantages; for instance, ZnO exhibits a higher absorption efficiency across a larger fraction of the solar spectrum when compared to TiO_2 [11], but it is more susceptible to photocorrosion [12]. On the other hand, TiO_2 has a lower charge mobility compared to ZnO, which leads to a higher recombination rate of electron–hole pairs [13]. Therefore, it is possible to assume that a heterojunction formed by both TiO_2 and ZnO might combine some of the appealing properties of both oxides.

For instance, Lun Pan et *al*. reported the synthesis of ~1 μm TiO_2 spheres decorated with nanometric ZnO clusters by a solvothermal method for the photocatalytic isomerization of norbornadiene [14]. Their results showed that higher photoactivities were obtained with the TiO_2/ZnO composite spheres compared to just using either pure TiO_2 or ZnO. Meanwhile, Ahsan Habib et al. [15] showed that by synthetizing ZnO/TiO_2 powders at different molar ratios for the photocatalytic degradation of dyes, their results showed higher degradations when both photocatalysts were mixed, with the most performing sample at a molar ratio of 3:1 ZnO/TiO_2. In addition, TiO_2/bentonite composites modified with ZnO showed enhanced performance with an optimal ZnO loading, achieving 95% methyl orange degradation [16]. Former examples are powdered photocatalysts that can be easily applied in slurry reactors.

Photocatalytic slurry reactors are commonly used at laboratory-scale or pilot-scale. Their main advantage is the high surface area of the powdered photocatalyst and the high mass transfer between the pollutants and the photocatalyst. However, their large-scale implementation is hindered by the post-treatment steps needed to retrieve the powdered-based photocatalyst from the water [17]. Moreover, powdered photocatalysts might cause light scattering that inhibits photocatalytic degradation rates [18]. Alternatively, photocatalyst immobilization on a solid support can overcome these disadvantages, allowing the recovery and reuse of the photocatalyst.

A wide variety of materials, such as glass [19], chitosan gel beads [20], clay beads [21], activated carbon [22], and calcium alginate beads [23], have been used as support materials. Glass materials often require surface pretreatment due to poor surface area and low durability [24]. Based on Wasidi's [25] research, chitosan gel beads are susceptible to swelling and dissolution under acidic conditions, which may result in structural instability and a progressive decline in adsorption performance. Repeated use of activated carbon in photocatalysis leads to residue accumulation, causing surface fouling that blocks active sites and lowers catalytic efficiency [26]. Among the aforementioned materials, clay beads have emerged as promising supports due to their low cost, low toxicity, high chemical stability, and mechanical strength [27, 28]. The properties of the support material can enhance the performance of a photocatalyst, as demonstrated by Manova, Aranda [29], who used the clay beads as a support for Degussa P25. However, despite these advantages, the development of stable and efficient TiO_2/ZnO composite immobilization on clay beads has not been systematically explored. This creates the necessity to investigate the photocatalytic efficiency and reusability of clay bead-supported photocatalysts.

Hence, the present work demonstrates the synthesis of two sets of TiO_2/ZnO composites supported on clay beads via the sol–gel dip coating method, offering a novel approach to enhance the photocatalytic degradation efficiency and reusability of immobilized photocatalysts. The first set involved a TiO_2 sol mixed with a ZnO sol, while the second set was a TiO_2 sol mixed with a commercially available powdered ZnO. The composites were characterized, and their photocatalytic performance was assessed. Finally, the reusability of the TiO_2/ZnO coated clay beads was evaluated by performing consecutive photocatalytic experiments.

2. Materials and methods

2.1. *TiO_2/ZnO composites sol preparation*

A detailed preparation procedure for both sets of composites is shown in Figure 1. For all the experiments, the TiO_2 sol was prepared at room temperature by dissolving titanium (IV) isopropoxide (Aldrich, 97%) in 2-propanol (Sigma-Aldrich, 99.5%).

The solution was continuously stirred for two hours to obtain the precursor solution. Then, a solution of distilled water and acetic acid (Sigma-Aldrich, ≥ 99.7%) was poured into the precursor solution at a speed of 1 drop/s under continuous stirring. Next, the solution was continuously stirred for 10 min to attain a yellow transparent sol. Later, acetylacetone (Emsure) was added and mixed for 30 min to increase the mixture stability.

The ZnO sol was prepared as follows: initially, zinc acetate dihydrate (HmbG Chemicals) was dissolved in ethanol (HmbG Chemicals, 95%) and stirred for 5 minutes at 70°C to obtain the precursor solution. Then, distilled water, ethanol, and diethanolamine (Emsure) were dropped into the precursor solution at a speed of 1 drop/s under vigorous stirring. The solution was continuously stirred for two hours to attain a transparent ZnO sol. Then, the prepared TiO_2 sol was directly added into the ZnO sol at different volume ratios of TiO_2:ZnO of 1:0, 3:1, 1:1, 1:3, and 0:1. For the second set of experiment, the fixed volume of TiO_2 sol was mixed with different amounts (1 to 5 g) of a commercially available powdered ZnO (R&M Chemicals) to obtain different ratios of TiO_2:ZnO.

2.2. *Catalyst immobilization*

The TiO_2/ZnO coated clay beads were prepared by the dip-coating method. Clay beads classified as light expanded clay aggregates (LECA) were used as a solid support for catalyst immobilization. Clay beads were washed a few times with water and acetone for 10 minutes before being dried in an oven at 100°C. Then, the clean clay beads were immersed in the freshly prepared TiO_2/ZnO sol at a speed of 1 mm/s.

Next, the dip-coated beads were allowed to air-dry for 5 minutes in the fume hood. Later, the coated clay beads were shifted to an oven at 100°C for 30 minutes. This procedure was repeated before the beads were placed into a furnace for calcination.

The conditions were 2°C/min up to 500°C and 1 h dwell time.

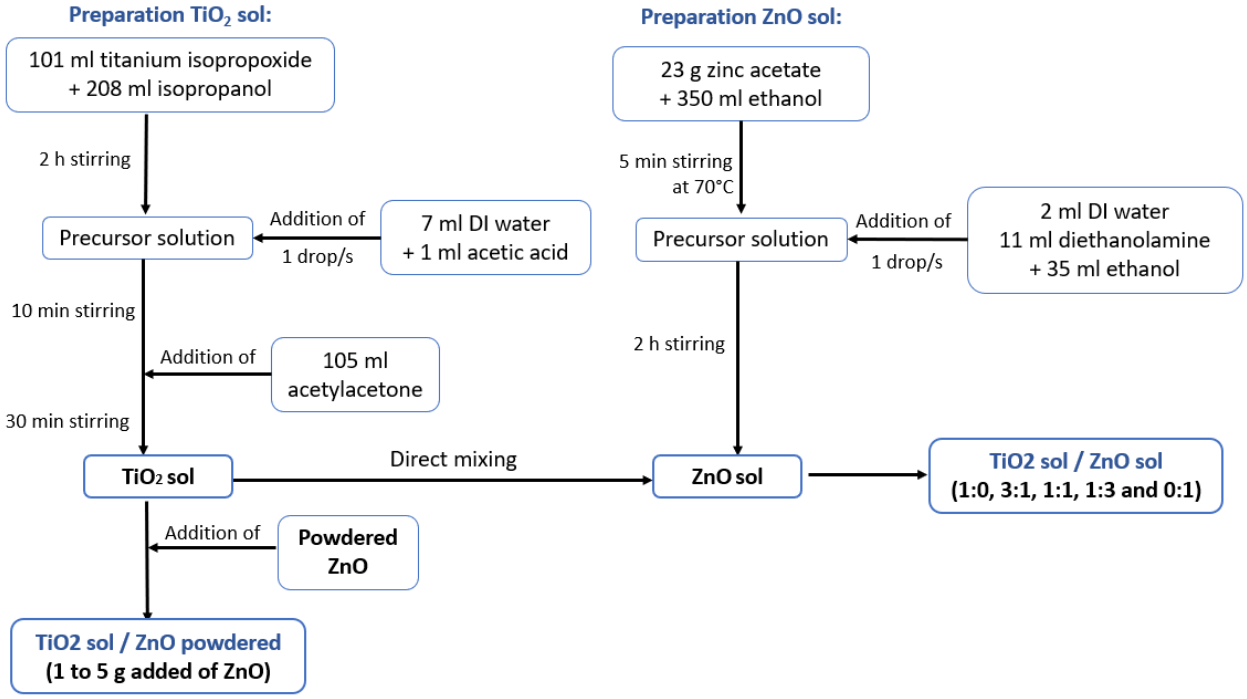

Fig. 1. Flowchart for the preparation of the TiO_2/ZnO composites.

The samples were left to cool down naturally. The procedure was repeated to acquire four TiO_2/ZnO layers, with a calcination step every two layers. The same preparation procedure was used for the set of samples prepared using the TiO_2 sol and the powdered ZnO.

2.3. *Characterization*

Scanning Electron Microscopy (model: JSM-6360 LA; JEOL) was used to obtain the morphology of the bare clay beads and the TiO_2/ZnO coated clay beads. Prior to the analysis, the samples were sputtered with gold (JFC-1600 Auto fine coater). An acceleration voltage of 20 kV was applied for the imaging of all samples. The surface elemental composition of the samples was acquired via EDS.

2.4. *Photocatalytic degradation experiments*

Photocatalytic experiments were conducted in a 500 mL column-shaped glass reactor equipped with a 13 W UV lamp (WK-X2) placed vertically inside the reactor (Figure 2).

The light source was positioned at the centre of the solution to ensure uniform irradiation. A limitation of this study is the absence of a direct irradiance measurement ($mW \cdot cm^{-2}$); however, lamp type, position, and reactor geometry were kept constants for all tests to ensure comparability.

A total volume of 500 mL of methylene blue (MB) solution (25 mg/L) was used, with a fixed amount of TiO_2/ZnO-coated clay beads. The suspension was continuously agitated at 1500 rpm using a magnetic stirrer to maintain homogeneous mixing and prevent sedimentation. All the experiments were carried out at room temperature (25 + 2^0C). The photocatalytic reactions were conducted for 180 min, and aliquots (5 mL) were withdrawn at predetermined time intervals. The concentration of MB was determined by UV-Vis spectrophotometry (UV-1800; Shimadzu) at the maximum absorption wavelength of 664 nm. The photocatalytic performance was evaluated in terms of degradation kinetics and degradation efficiency studies. The degradation rate followed pseudo-first-order kinetics and was calculated by the following equation:

$$\ln (C/Co) = -k \times t \quad (1)$$

The degradation efficiency was calculated as follows:

$$\% \text{ Degradation} = [C0-Ct] / C0 \times 100\% \quad (2)$$

where k is the pseudo-first-rate kinetic constant, C_o is the initial concentration, and C is the concentration of methylene blue at time, t.

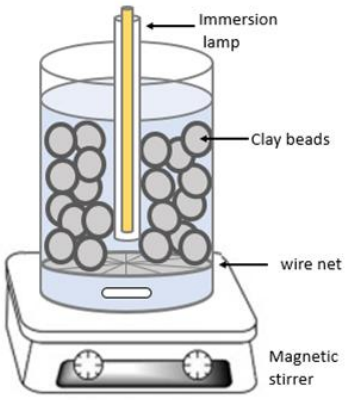

Fig. 2. Experimental setup of the photocatalytic reactor.

2.5. *Statistical analysis*

A two-way analysis of variance (ANOVA) without replication at $P < 0.05$ was used to analyse the results using Microsoft excel package 2021.

3. Results and discussion

3.1. Synthesis and characterization of the $TiO_{2(sol)}$/$ZnO_{(sol)}$-coated clay beads

A series of TiO_2/ZnO composites were successfully prepared by the direct mixing of a TiO_2 sol with a ZnO sol at different volume ratios, as described in Figure 1. SEM-EDS was used to obtain information about the morphological features and to acquire the elemental composition of both the bare clays beads and the $TiO_{2(sol)}$/$ZnO_{(sol)}$ coated beads; the results are shown in Figure 3 and Table 1, respectively. The SEM micrographs of the bare clay beads show a rough and non-porous surface (Figure 3a). Meanwhile, the EDS analysis (Table 1) indicated the presence of a wide variety of elements, K, Mg, Ca, Al, Fe, Si, and O. These results are expected because clays consist of tetrahedral silica sheets and octahedral sheets of either gibbsite, $Al(OH)_3$ or brucite, $Mg(OH)_2$, stacked upon each other [30]. The rest of the elements are commonly found on clays [31]. Figure 3b shows the TiO_2 crystalline structures obtained over the surface of the bare clay beads after the calcination process. The micrograph shows complete coverage of the clay bead´s surface and the formation of

crystalline structures. The EDS analysis (Table 1) detects the signal of titanium and oxygen from the TiO_2, as well as the signal of some elements that form the clay beads. A previous report on the synthesis of TiO_2 by the sol–gel route using acetylacetone as a stabilizing agent showed the formation of crystalline structures of anatase TiO_2 [32], similar to the ones obtained in the present work.

The SEM micrographs of the coated clay beads produced by mixing the $TiO_{2(sol)}$ and the $ZnO_{(sol)}$ at different ratios are illustrated in Figure 3c to Figure 3e. The micrographs show a complete change in the morphology of the coated clay beads, as the amount of ZnO increased. Firstly, it was observed that the formation of the TiO_2 crystal structure was inhibited by the incorporation of ZnO [33]. The EDS analysis of the different $TiO_{2(sol)}/ZnO_{(sol)}$ samples confirmed the presence of both ZnO and TiO_2 over the surface of the clay beads. Furthermore, the SEM micrograph of the pure ZnO coated clay beads (Figure 3f) shows the formation of ZnO nanoparticles that were evenly distributed over the surface of the clay bead. For this sample, the EDS analysis detected the signal of zinc and oxygen from the ZnO, and the signal of other elements that form the clay beads.

3.2. *Synthesis and characterization of the $TiO_{2(sol)}/ZnO_{(powdered)}$-coated clay beads*

Another set of TiO_2/ZnO composites was prepared by direct mixing of TiO_2 sol with different amounts of commercially available ZnO powder (from 1 to 5 g). The obtained solution was coated on the bare clay beads, as described in Section 2.2.

The SEM micrographs of the $TiO_{2(sol)}/ZnO_{(powdered)}$ are displayed in Figure 4a to Figure 4e. Images show a similar morphology for all the samples, which is characterized by a compact structure and the formation of cracks. Table 2 shows the EDS analysis of each sample.

The results showed that the mass percentages of Zn increased with the amount of powdered ZnO added. The EDS analysis confirmed the presence of Ti, O, and Zn, along with elements from the clay beads, indicating successful immobilization of TiO_2/ZnO composites on clay beads. Similar findings has been reported, where EDS validated the uniform distribution of active elements within hybrid nanocomposites [34].

3.3. *Photocatalytic activities of $TiO_{2(sol)}/ZnO_{(sol)}$ coated clay beads*

The performance of the coated clay beads obtained by the $TiO_{2(sol)}/ZnO_{(sol)}$ and the $TiO_{2(sol)}/ZnO_{(powdered)}$ was assessed by the photocatalytic degradation of methylene blue (MB). The photocatalytic experiments were conducted for three hours, and the results are displayed in Figure 5a and 5b. The pure TiO_2-coated clay beads outperformed all the TiO_2/ZnO composites, achieving a degradation efficiency of 96.8%. Comparable efficiencies have also been reported using a rod-like $[Cu(phen)_2(OAc)]PF_6$ complex, which exhibited 90.1% MB photocatalytic degradation performance under visible light irradiation [35]. The degradation performances of all $TiO_{2(sol)}/ZnO_{(sol)}$ coated clay beads ranged from 65% to 83%.

The best performance was achieved for the sample with the composition of 50:50 $TiO_{2(sol)}/ZnO_{(sol)}$, achieving a degradation efficiency of 83%. The photodegradation process was fit for a pseudo-first-order kinetics with the apparent rate constant, k, of the TiO_2, and the 50:50 TiO_2/ZnO coated beads were 18.2×10^{-3} min^{-1} and 10.1×10^{-3} min^{-1}, respectively. Figure 5a illustrates the apparent rate constant, k, for all $TiO_{2\ (sol)}/ZnO_{\ (sol)}$ composites.

3.4. *Photocatalytic activities of $TiO_{2\ (sol)}/ZnO_{\ (powdered)}$ coated clay beads*

Photocatalytic degradation experiments using a fixed amount of TiO_2 were also performed, while varying the loading of a commercially available powdered ZnO (1–5 g). The aim of this set of experiments was to evaluate the effect of the concentration of ZnO on the photocatalytic performance; the results are shown in Figure 5b. TiO_2-coated clay beads had higher degradation efficiencies than the $TiO_{2(sol)}/ZnO_{(powdered)}$-coated beads, which had degradation efficiencies ranging from 65% to 88%. The most performing composite corresponded to the sample prepared by adding 3 g of powdered ZnO to the TiO_2 sol. The lowest photocatalytic degradation rate recorded was 6.5×10^{-3} min^{-1} for the composite TiO_2:1 g ZnO. A slightly higher apparent rate constant, k, was observed for all composites prepared using powdered ZnO compared to the samples synthesized using ZnO sol.

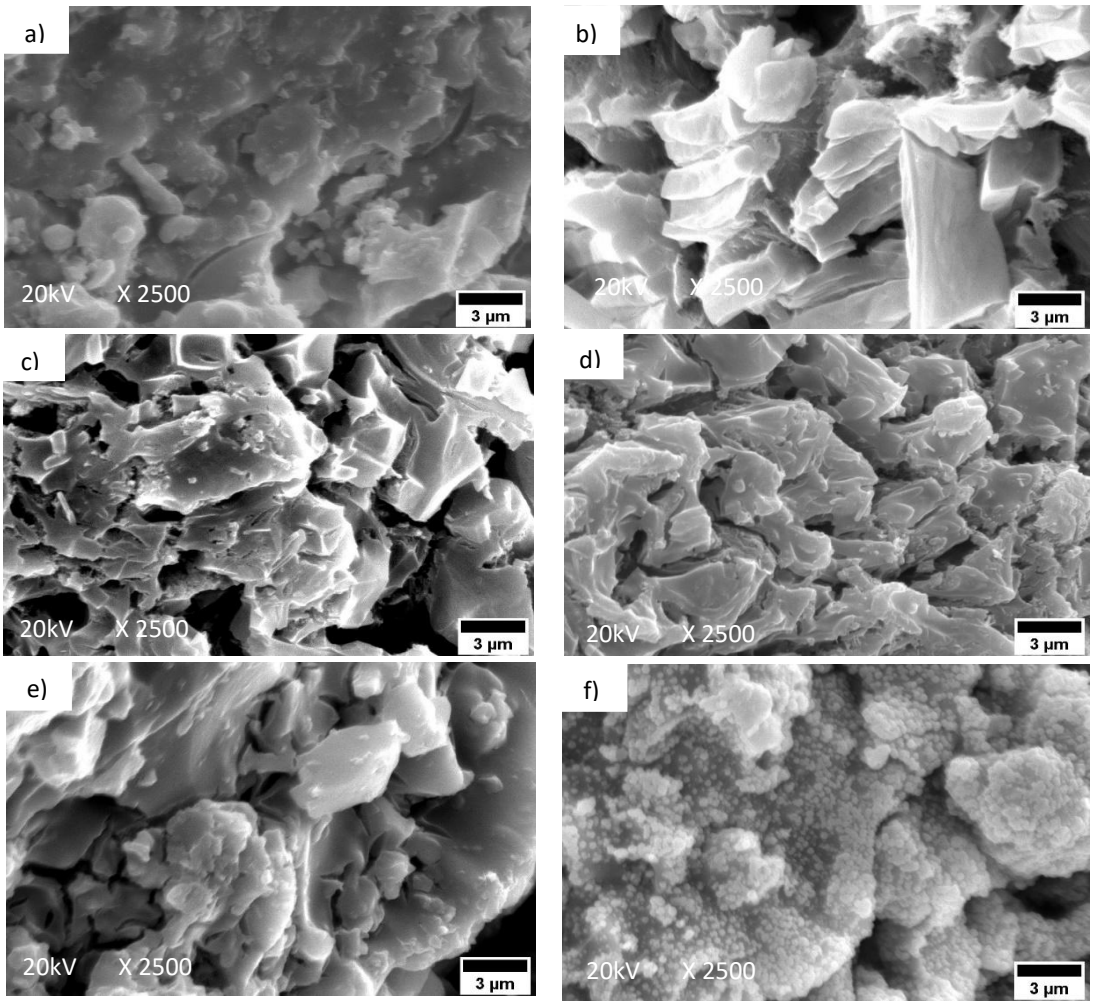

Fig. 3. SEM micrographs of the: a) bare clay beads and the coated clay beads with TiO_2(sol)/ZnO(sol) at different volume ratios of: b) 1:0; c) 3:1; d) 1:1; e) 1:3; and f) 0:1.

Table 1. EDS analysis of the bare clay beads and coated by $TiO_{2(sol)}$:$ZnO_{(sol)}$.

	K	Mg	Ca	Al	Fe	Si	Ti	Zn	O
Bare clays beads	2.03	1.02	1.44	9.07	21.50	22.17	-	-	41.74
$TiO_{2(sol)}$:$ZnO_{(sol)}$ ratio:									
100:0	0.66	-	0.75	2.43	6.86	5.75	43.19	-	40.06
75:25	0.74	-	0.40	4.50	6.16	6.19	36.69	5.47	39.19
50:50	0.63	-	0.73	2.47	8.1:1	5.32	27.33	19.79	34.58
25:75	1.81	-	0.96	9.32	10.60	19.33	4.55	23.02	40.61
0:100	1.30	-	2.29	7.28	12.22	16.37	-	23.40	36.07

Table 2. EDS analysis of the bare and coated clay beads with $TiO_{2(sol)}$:$ZnO_{(powdered)}$.

	K	Mg	Ca	Al	Fe	Si	Ti	Zn	O
Bare clays beads	2.03	1.02	1.44	9.07	21.50	22.17	-	-	41.74
$TiO_{2(sol)}$:$ZnO_{(powdered)}$									
TiO_2:1 g	1.30	-	0.68	1.89	1.97	3.53	42.63	5.12	42.88
TiO_2:2 g	0.94	-	1.05	1.49	1.76	2.40	28.56	13.76	50.05
TiO_2:3 g	1.53	-	0.22	1.34	1.66	2.80	34.75	16.13	41.56
TiO_2:4 g	1.03	-	0.33	1.03	2.35	1.73	46.41	17.87	29.25
TiO_2:5 g	2.03	-	1.17	2.02	3.84	4.17	32.04	19.23	35.50

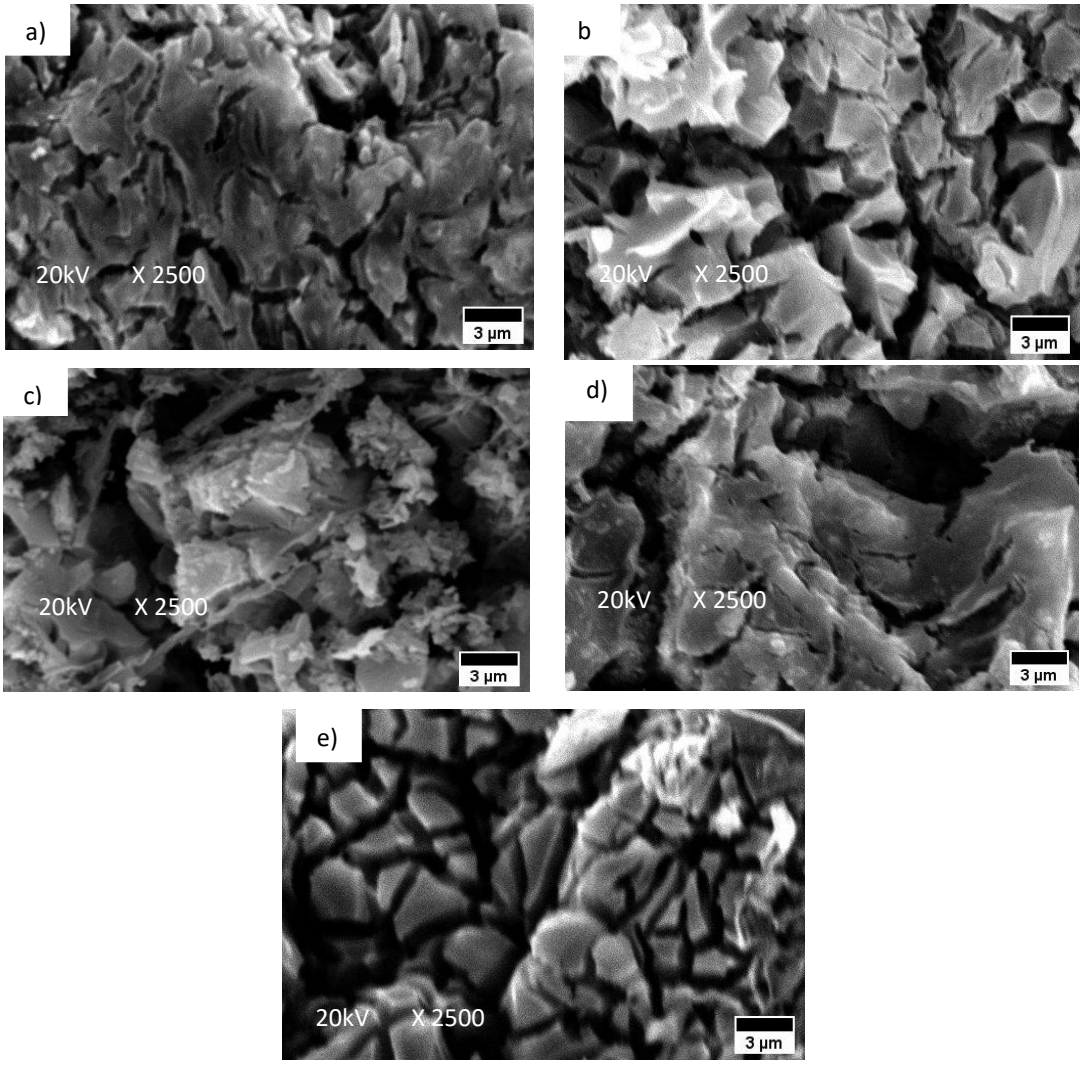

Fig. 4. SEM analysis of the coated clay beads with different TiO_2(sol)/ZnO(powdered) by adding different amounts of ZnO at: a) 1 g; b) 2 g; c) 3 g; d) 4 g; and e) 5 g.

Similar improvements in degradation efficiency using hybrid catalyst systems have been reported; for example, Rajabi *et Al*. [36] achieved an 82.9% removal rate for monoethylene glycol by Ag^{0}/CuO-doped in the presence of persulfate and ultrasonic waves.

3.5. *Recycling performance of $TiO_{2(sol)}/ZnO_{(sol)}$ and $TiO_{2(sol)}/ZnO_{(powdered)}$-coated clay beads*

The major advantages of immobilizing a photocatalyst are its reusability and easy retrieval from water. Therefore, supporting materials should meet specific requirements, such as high specific area, environmentally friendly nature, as well as strong and durable bonding with the catalyst [37]; clay beads could meet these requirements.

Recyclability experiments were performed on all coated clay beads. Five consecutive photocatalytic degradation experiments were performed under the same conditions. Figure 5c demonstrates the results for the TiO_2(sol)/ZnO(sol), while Figure 5d shows that for the TiO_2(sol)/ZnO(powdered). On the other hand, Table 3 reports the average degradation efficiencies and average reaction rates for the five experiments.

The five consecutive experimental results show similar degradation efficiencies. The highest average degradation rate of the pure TiO_2-coated beads was 96.5 ± 0.58%, with an average reaction rate of 19.3×10^{-3} min^{-1} (Table 3). On the other hand, the average degradation efficiency of the pure $ZnO_{(sol)}$ coated clay beads was 76.8 ± 5.1%, with a $k = 8.2 \times 10^{-3}$ min^{-1}, which is close to the average degradation efficiencies of all $TiO_{2(sol)}/ZnO_{(sol)}$ composites (72.8%–77.4%). Figure

5d and Table 3 show the recyclability experiments for the $TiO_{2(sol)}/ZnO_{(powdered)}$-coated clay beads. These results indicate slightly higher degradation efficiencies were achieved by the $TiO_{2(sol)}/ZnO_{(powdered)}$ (72.2%–87.1%) compared to the values obtained for the $TiO_{2(sol)}/ZnO_{(sol)}$ (72.8%–77.4%).

The results indicate the coating procedure was successfully carried out, either by using the ZnO synthesized by the sol–gel method or by using the commercially available powdered ZnO, and that all composites managed to maintain their photocatalytic performances after five cycles. A limitation of this study is the absence of direct measurements of photocatalyst leaching. However, there is no turbidity or visible catalyst residues observed in the solution, suggesting negligible detachment. The clay beads also retained their structural integrity during reuse. These qualitative observations align with previous works, where TiO_2 nanoparticles immobilized on mortar spheres maintained over 83% of aniline blue photocatalytic decolorization efficiency across twenty consecutive cycles [38].

3.6. *Statistical analysis results of $TiO_{2(sol)}/ZnO_{(sol)}$ and $TiO_{2(sol)}/ZnO_{(powdered)}$-coated clay beads*

A two-way analysis of variance (ANOVA) without replication at a 0.05 significance level was performed to describe the relationships between (1) TiO_2: ZnO ratio and variation of time, and (2) methylene blue degradation efficiency. The results are presented in Table 4. The data ($TiO_{2(sol)}/ZnO_{(sol)}$) shows the p-value for the ratio = 2.98E-12 < 0.05 = α (or F = 61.35 > 2.78 = F-crit) and the p-value for the time = 3.17E-18 < 0.05 = α (or F = 162.70 > 2.51 = F-crit).

So, at the 95% level of confidence, we conclude there is a significant difference between the $TiO_{2(sol)}/ZnO_{(sol)}$ ratio and time with the methylene blue degradation efficiency.

The data ($TiO_{2(sol)}/ZnO_{(powdered)}$) shows the p-value for the ratio = 5.37E-06 < 0.05 = α (or F = 10.77 > 2.53 = F-crit) and the p-value for the time = 3.65E-18 < 0.05 = α (or F = 95.23 > 2.42 = F-crit). So, at the 95% level of confidence, we conclude there is a significant difference between the $TiO_{2(sol)}/ZnO_{(powdered)}$ ratio and time with the methylene blue degradation efficiency.

Table 3. Average degradation efficiencies after five consecutive experiments and average degradation rates for the $TiO_{2(sol)}/ZnO_{(sol)}$ and the $TiO_{2(sol)}/ZnO_{(powdered)}$.

$TiO_{2(sol)}/ZnO_{(sol)}$	**Average degradation efficiency/%**	**Degradation rate/k*10^{-3} min^{-1}**	**$TiO_{2(sol)}/ZnO_{(powdered)}$**	**Average degradation efficiency/%**	**Degradation rate/k*10^{-3} min^{-1}**
100:0	96.5 ± 0.6	19.3	TiO_2: 1 g ZnO	72.2 ± 5.7	7.4
75:25	72.8 ± 5.4	7.2	TiO_2: 2 g ZnO	83.3 ± 0.5	10.1
50:50	77.4 ± 7.0	8.4	TiO_2: 3 g ZnO	87.1 ± 1.0	11.5
25:75	74.5 ± 1.7	7.4	TiO_2: 4 g ZnO	79.3 ± 0.7	8.2
0:100	76.8 ± 5.1	8.2	TiO_2: 5 g ZnO	77.9 ± 1.4	8.1

Table 4. Two-way analysis of variance (ANOVA) without replication for the degradation efficiency.

Source of Variation	*SS*	*df*	*MS*	*F*	*P-value*	*F crit*
$TiO_{2(sol)}/ZnO_{(sol)}$						
Ratio	4305.354	4	1076.339	61.35076	2.98E-12	2.776289
Time	17126.72	6	2854.454	162.7024	3.17E-18	2.508189
Error	421.0563	24	17.54401			
Total	21853.13	34				
$TiO_{2(sol)}/ZnO_{(powdered)}$						
Ratio	1534.338	5	306.8676	10.77222	5.37E-06	2.533555
Time	16276.14	6	2712.689	95.2257	3.65E-18	2.420523
Error	854.6083	30	28.48694			
Total	18665.08	41				

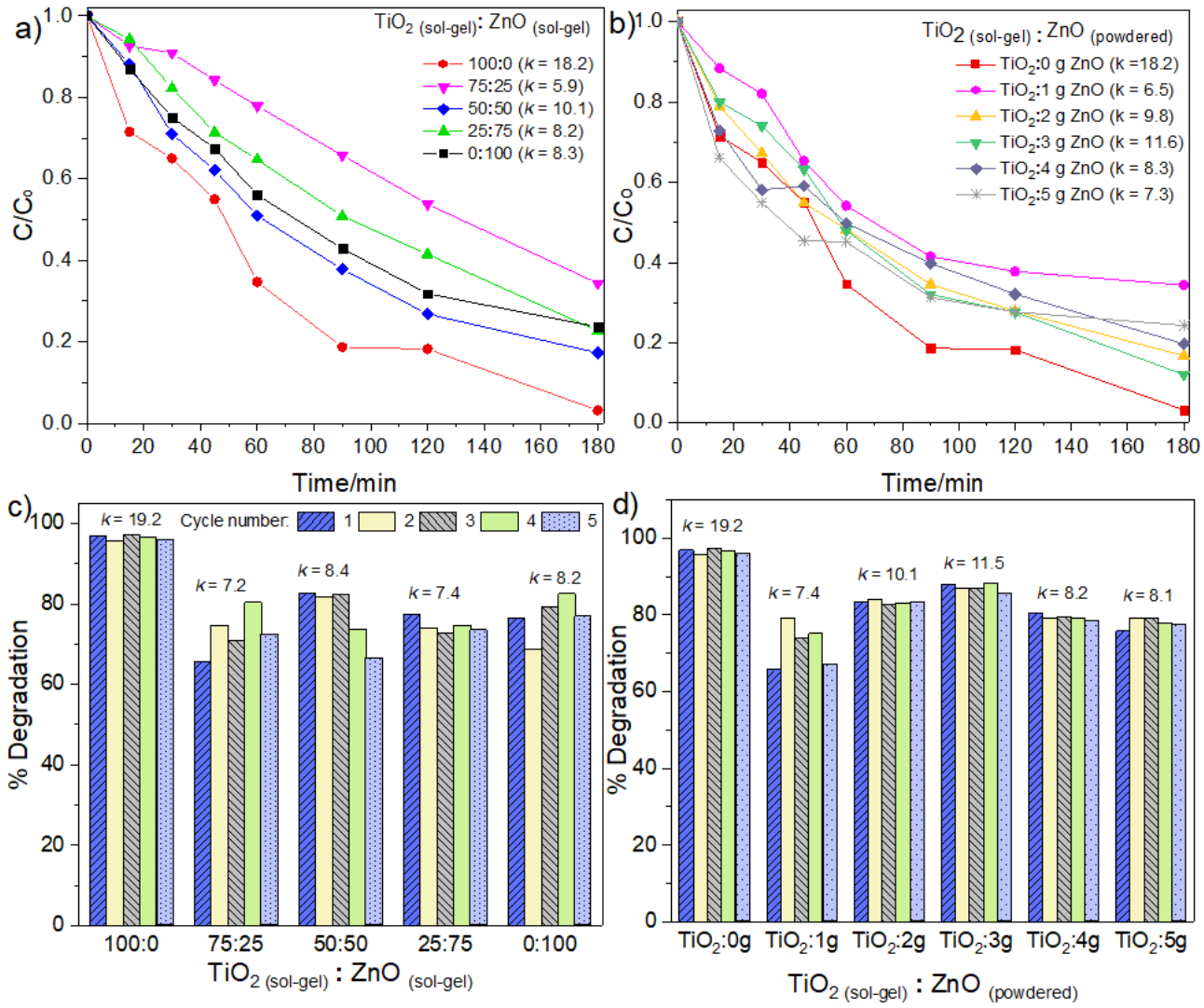

Fig. 5. Degradation experiments for the coated clay beads prepared with a) $TiO_{2(sol)}/ZnO_{(sol)}$ and b) $TiO_{2(sol)}/ZnO_{(powdered)}$. The recyclability experiments are conducted for: c) $TiO_{2(sol)}/ZnO_{(sol)}$ and d) $TiO_{2(sol)}/ZnO_{(powdered)}$. Degradation rate, *k*, is expressed as $\times 10^{-3}$ min^{-1}.

4. Conclusion

Different TiO_2/ZnO composites were successfully synthesized via the sol–gel method and immobilized on clay beads using a dip-coating process. Among the composites, $TiO_{2(sol)}/ZnO_{(powdered)}$ was identified as the most effective hybrid photocatalyst. The porosity and adsorption properties of the clay beads enabled the deposition of multiple photocatalyst layers, while the addition of $ZnO_{(powdered)}$ increased the viscosity of the TiO_2 sol, facilitating uniform coating. Photocatalytic evaluation under UV irradiation showed that pure TiO_2 achieved the highest degradation efficiency of 96.5%, whereas TiO_2/ZnO-coated beads exhibited efficiencies between 65.7% and 88.0%. All the samples maintained their photocatalytic performance over five consecutive reuse cycles, indicating stable immobilization and minimal deactivation. A limitation of this study is the absence of direct measurements of photocatalyst leaching and coating integrity.

Future work should include quantitative analyses of leaching and long-term structural stability to further validate the practical applicability of immobilized materials. Overall, the use of low-cost, mechanically stable clay-supported TiO_2/ZnO

composites with reliable reusability highlights their potential for cost-effective scale-up and practical implementation in large-scale wastewater treatment systems.

Author's contribution

Thurgadewi Krishnan: Investigation, Formal analysis, Writing – original draft; Maria Medina-Llamas: Writing – review and editing; Mohamad Awang: Writing – review and editing; Wan Rafizah Wan Abdullah: Writing – review and editing; Wan Salida Wan Mansor: Conceptualization, Methodology, Supervision, Writing – review and editing.

Conflict of interest

No potential conflict of interest was reported by the authors.

Data availability

Not Applicable.

Funding

This work was supported by Universiti Malaysia Terengganu (UMT/TAPE-RG/2020/55247).

References

[1] El Nemr, A., Helmy, E. T., Gomaa, E. A., Eldafrawy, S., & Mousa, M. (2019). Photocatalytic and biological activities of undoped and doped TiO_2 prepared by green method for water treatment. *Journal of Environmental Chemical Engineering*, *7*, 103385. https://doi.org/10.1016/j.jece.2019.103385

[2] Moorthy, A. K., Rathi, B. G., Shukla, S. P., Kumar, K., & Bharti, V. S. (2021). Acute toxicity of textile dye methylene blue on growth and metabolism of selected freshwater microalgae. *Environmental Toxicology and Pharmacology*, *82*, 103552. https://doi.org/10.1016/j.etap.2020.103552

[3] Haider, A. J., Jameel, Z. N., & Al-Hussaini, I. H. (2019). Review on: Titanium dioxide applications. *Energy Procedia*, *157*, 17–29. https://doi.org/10.1016/j.egypro.2018.11.159

[4] Rayati, S., Bathaee, H., & Badiei, A. (2024). Catalytic activity of Fe/Mn porphyrins grafted on graphitic carbon nitride in the heterogeneous oxidation of olefins. *Applied Organometallic Chemistry*, *38*(11). https://doi.org/10.1002/aoc.7679

[5] Slama, H. B., Bouket, A. C., Pourhassan, Z., Alenezi, F. N., Silini, A., Cherif-Silini, H., & Belbahri, L. (2021). Diversity of synthetic dyes from textile industries, discharge impacts and treatment methods. *Applied Sciences*, *11*, 6255. https://doi.org/10.3390/app11146255

[6] Khan, I., Saeed, K., Zekker, I., Zhang, B., Hendi, A. H., Ahmad, A., & Ahmad, S., et al. (2022). Review on methylene blue: Its properties, uses, toxicity and photodegradation. *Water*, *14*(2), 242. https://doi.org/10.3390/w14020242

[7] Zamel, D., & Khan, A. U. (2021). Bacterial immobilization on cellulose acetate-based nanofibers for methylene blue removal from wastewater: Mini-review. *Inorganic Chemistry Communications*, *131*, 108766. https://doi.org/10.1016/j.inoche.2021.108766

[8] Mirhosseyni, M. S., Mohammadi Ziarani, G., & Badiei, A. (2025). Catalytic development of boron and sulphur-doped g-C_3N_4 supported Cu-MOF composite for nitroarenes reduction reaction. *Journal of Molecular Structure*, *1321*, 139763. https://doi.org/10.1016/j.molstruc.2024.139763

[9] Malekshahi Byranvand, M., Nemati Kharat, A., Fatholahi, L., & Malekshahi Beiranvand, Z. (2013). A review on synthesis of nano-TiO_2 via different methods. *Journal of Nanostructures*, *3*(1), 1–9. https://doi.org/10.7508/jns.2013.01.001

[10] Pirhashemi, M., Habibi-Yangjeh, A., & Pouran, S. R. (2018). Review on the criteria anticipated for the fabrication of highly efficient ZnO-based visible-light-driven photocatalysts. *Journal of Industrial and Engineering Chemistry*, *62*, 1–25. https://doi.org/10.1016/j.jiec.2018.01.012

[11] Qiu, R., Zhang, D., Mo, Y., Song, L., Brewer, E., Huang, X., & Xiong, Y. (2008). Photocatalytic activity of polymer-modified ZnO under visible light irradiation. *Journal of Hazardous Materials*, *156*, 80–85. https://doi.org/10.1016/j.jhazmat.2007.11.114

[12] Taylor, C. M., Ramirez-Canona, A., Wenk, J., & Mattia, D. (2019). Enhancing the photo-

corrosion resistance of ZnO nanowire photocatalysts. *Journal of Hazardous Materials*, *378*, 120799. https://doi.org/10.1016/j.jhazmat.2019.120799

[13] Daghrir, R., Drogui, P., & Robert, D. (2013). Modified TiO_2 for environmental photocatalytic applications: A review. *Industrial & Engineering Chemistry Research*, *52*(10), 3581–3599. https://doi.org/10.1021/ie303468t

[14] Pan, L., Shen, G.-Q., Zhang, J. W., Wei, X. C., Li, Wang, J. J., Xou, X., & Zhang, X. (2015). TiO_2–ZnO composite sphere decorated with ZnO clusters for effective charge isolation in photocatalysis. *Industrial & Engineering Chemistry Research*, *54*(18), 7226–7232. https://doi.org/10.1021/acs.iecr.5b01471

[15] Habib, M. A., Shahadat, M. T., Bahadur, N. M., Ismail, I. M. I., & Mahmood, A. J. (2013). Synthesis and characterization of ZnO-TiO_2 nanocomposites and their application as photocatalysts. *International Nano Letters*, *3*, 5. https://doi.org/10.1186/2228-5326-3-5

[16] Dinari, A., & Mahmoudi, J. (2022). Response surface methodology analysis of the photodegradation of methyl orange dye using synthesized TiO_2/Bentonite/ZnO composites. *Advances in Environmental Technology*, *1*, 31–46. https://doi.org/10.22104/AET.2022.5204.1409

[17] Azha, S. F., Shahadat, M., Ismail, S., Ali, S. W., & Ahammad, S. Z. (2021). Prospect of clay-based flexible adsorbent coatings as cleaner production technique in wastewater treatment, challenges, and issues: A review. *Journal of the Taiwan Institute of Chemical Engineers*, *120*, 178–206. https://doi.org/10.1016/j.jtice.2021.03.018

[18] Srikanth, B., Goutham, R., Narrayan, R. B., Ramprasath, A., Gopinath, K. P., & Sankaranarayanan, A. R. (2017). Recent advancements in supporting materials for immobilised photocatalytic applications in wastewater treatment. *Journal of Environmental Management*, *200*, 60–78. https://doi.org/10.1016/j.jenvman.2017.05.063

[19] Hakki, H. K., Allahyari, S., Rahemi, N., & Tasbihi, M. (2019). Surface properties, adherence, and photocatalytic activity of sol–gel dip-coated TiO_2–ZnO films on glass plates. *Comptes Rendus Chimie*, *22*(6), 393–40. https://doi.org/10.1016/j.crci.2019.05.007

[20] Anusuya, N., Pragathiswaran, C., & Mary, J. V. (2021). A potential catalyst-TiO_2/ZnO based chitosan gel beads for the reduction of nitro-aromatic compounds aggregated sodium borohydride and their antimicrobial activity. *Journal of Molecular Structure*, *1236*, 130197. https://doi.org/10.1016/j.molstruc.2021.130197

[21] Iazdani, F., & Nezamzadeh-Ejhieh, A. (2021). The photocatalytic rate of ZnO supported onto natural zeolite nanoparticles in the photodegradation of an aromatic amine. *Environmental Science and Pollution Research*, *28*, 53314–53327. https://doi.org/10.1007/s11356-021-14544-8

[22] Hung, M. C., Yuan, S. Y., Hung, C. C., Cheng, C. L., Ho, H. C., & Ko, T. H. (2014). Effectiveness of ZnO/carbon-based material as a catalyst for photodegradation of acrolein. *Carbon*, *66*, 93–104. https://doi.org/10.1016/j.carbon.2013.08.047

[23] Isik, Z., Bilici, Z., Adiguzel, S. K., Yatmaz, H. C., & Dizge, N. (2019). Entrapment of TiO_2 and ZnO powders in alginate beads: Photocatalytic and reuse efficiencies for dye solutions and toxicity effect for DNA damage. *Environmental Technology & Innovation*, *14*, 100358. https://doi.org/10.1016/j.eti.2019.100358

[24] Tian, S., Feng, Y., Zheng, Z., & He, Z. (2023). TiO_2-based photocatalytic coatings on glass substrates for environmental applications. *Coatings*, *13*(8), 1472. https://doi.org/10.3390/coatings13081472

[25] Al-Wasidi, A. S., Ahmed, M. A., Ahmed, H. A., Mahmoud, S. A., & Mohamed, A. A. (2025). Enhanced indigo carmine dye removal via chitosan-modified NiO-g-C_3N_4 catalyst: Adsorption and photocatalysis studies. *International Journal of Biological Macromolecules*, *320*, 145669. https://doi.org/10.1016/j.ijbiomac.2025.145669

[26] Osman, H., Yılmaz, S. I., Uğurlu, M., Vaizogullar, A. I., & Chaudhary, A. J. (2025). Synthesis and characterisation of activated carbon supported catalysts: Photocatalytic degradation of olive wastewater solutions

using these catalysts. *Journal of Sol-Gel Science and Technology*. Advance online publication. https://doi.org/10.1007/s10971-025-06833-2

[27] Han, H., Rafiq, M. K., Zhou, T., Xu, R., Masek, O., & Li, X. (2019). A critical review of clay-based composites with enhanced adsorption performance for metal and organic pollutants. *Journal of Hazardous Materials*, *369*, 780–796. https://doi.org/10.1016/j.jhazmat.2019.02.003

[28] Kamarudin, N. S., Jusoh, R., Setiabudi, H. D., Sukor, N. F., & Shariffuddin, J. H. (2021). Potential nanomaterials application in wastewater treatment: Physical, chemical and biological approaches. *Materials Today: Proceedings*, *42*, 107–114. https://doi.org/10.1016/j.matpr.2020.10.221

[29] Manova, E., Aranda, P., Martín-Luengo, M. A., Letaïef, S., & Ruiz-Hitzky, E. (2010). New titania-clay nanostructured porous materials. *Microporous and Mesoporous Materials*, *131*(1–3), 252–260. https://doi.org/10.1016/j.micromeso.2009.12.031

[30] Mishra, A., Mehta, A., & Basu, S. (2018). Clay supported TiO_2 nanoparticles for photocatalytic degradation of environmental pollutants: A review. *Journal of Environmental Chemical Engineering*, *6*(5), 6088–6107. https://doi.org/10.1016/j.jece.2018.09.029

[31] Mueller, B. (2015). Experimental interactions between clay minerals and bacteria: A review. *Pedosphere*, *25*(6), 799–810. https://doi.org/10.1016/S1002-0160(15)30061-8

[32] Verma, A., Samanta, S. B., Bakhshi, A. K., & Agnihotry, S. A. (2005). Effect of stabilizer on structural, optical and electrochemical properties of sol–gel derived spin coated TiO_2 films. *Solar Energy Materials and Solar Cells*, *88*(1), 47–64. https://doi.org/10.1016/j.solmat.2004.10.006

[33] Munguti, L., & Dejene, F. (2021). Effects of Zn:Ti molar ratios on the morphological, optical and photocatalytic properties of ZnO–TiO_2 nanocomposites for application in dye removal. *Materials Science in Semiconductor Processing*, *128*, 105786. https://doi.org/10.1016/j.mssp.2021.105786

[34] Rajabi, S., Hashemi, H., Samaei, M. R., Nasiri, A., Azhdarpoor, A., Yousefinejad, S., & Sartaj, M. (2024). Enhanced sonophoto-catalytic and adsorption capabilities of Fe_3O_4@MC/MWCNT-CuO/Ag for petrochemical organic pollutants degradation from industrial process streams. *Arabian Journal of Chemistry*, *17*(11), 105994. https://doi.org/10.1016/j.arabjc.2024.105994

[35] Zinatloo-Ajabshir, S., Rakhshani, S., Mehrabadi, Z., Farsadrooh, M., Feizi-Dehnayebi, M., Rakhshani, S., Dušek, M., Eigner, V., Rtimi, S., & Aminabhavi, T. M. (2024). Novel rod-like $[Cu(phen)_2(OAc)]\cdot PF_6$ complex for high-performance visible-light-driven photocatalytic degradation of hazardous organic dyes: DFT approach, Hirshfeld and fingerprint plot analysis. *Journal of Environmental Management*, *350*, 119545. https://doi.org/10.1016/j.jenvman.2023.119545

[36] Rajabi, S., Hashemi, H., Samaei, M. R., Nasiri, A., Azhdarpoor, A., Yousefinejad, S., Sartaj, M., & Isazadeh, S. (2025). Magnetic Ag^0 and CuO-doped bio-sonocatalyst multi-walled carbon nanotube for synergized degradation of monoethylene glycol from gas refinery effluents. *Journal of Water Process Engineering*, *77*, 108330. https://doi.org/10.1016/j.jwpe.2025.108330

[37] Bansal, P., & Verma, A. (2017). Synergistic effect of dual process (photocatalysis and photo-Fenton) for the degradation of cephalexin using TiO_2 immobilized novel clay beads with waste fly ash/foundry sand. *Journal of Photochemistry and Photobiology A: Chemistry*, *342*, 131–142. https://doi.org/10.1016/j.jphotochem.2017.04.010

[38] Cob-Cantú, J. R., Lopez-Velazquez, K., Ronderos-Lara, J. G., Hoil-Canul, E. R., Castillo-Quevedo, C., Maldonado-Lopez, L. A., & Cabellos-Quiroz, J. L. (2025). TiO_2 nanoparticles immobilized on mortar spheres as a strategy for efficient photocatalyst reuse: New UV reactor design for dye removal. *Frontiers in Chemistry*, *13*, 1581274. https://doi.org/10.3389/fchem.2025.1581274

How to cite this paper:

Krishnan, T., Llamas, M. M., Awang, M., Wan Abdullah, W. R. & Wan Mansor, W. S. (2026). Titanium Dioxide Sol–Gel/Zinc Oxide Sol–Gel and Titanium Dioxide Sol–Gel/Powdered Zinc Oxide-Coated Clay Beads in Photocatalytic Reactor. *Advances in Environmental Technology*, 12(3), 328-340. DOI: 10.22104/aet.2026.7628.2146